SCIENCE CHINA
Information Sciences

• LETTER •

June 2023, Vol. 66 169405:1–169405:2
https://doi.org/10.1007/s11432-022-3547-9

# Low-bias, high-photoresponsivity $SnSe_2$ nanofilm with an Au split-ring array-based THz detector toward 6G communication

Qi SONG[1,2], Zhiwen ZHOU[1], Yifei XU[1], Min ZHANG[1*], Junbo YANG[3],
Huawei LIANG[1], Tianwu WANG[4] & Peiguang YAN[1*]

[1]*College of Physics and Optoelectronic Engineering, Shenzhen University, Shenzhen* 518060*, China;*
[2]*Shandong Key Laboratory of Optical Communication Science and Technology,*
*School of Physics Science and Information Technology, Liaocheng University, Liaocheng* 252059*, China;*
[3]*College of Liberal Arts and Sciences, National University of Defense Technology, Changsha* 410073*, China;*
[4]*GBA Research Institute, Aerospace Information Research Institute of Chinese Academy of Science,*
*Guangzhou* 510725*, China*

Received 9 January 2022/Revised 26 April 2022/Accepted 8 July 2022/Published online 4 April 2023

**Citation** Song Q, Zhou Z W, Xu Y F, et al. Low-bias, high-photoresponsivity $SnSe_2$ nanofilm with an Au split-ring array-based THz detector toward 6G communication. Sci China Inf Sci, 2023, 66(6): 169405, https://doi.org/10.1007/s11432-022-3547-9

6G technology with the four characteristics of an intelligent endogenous, secure endogenous, multi-domain convergence, and integrated computing network, will help society toward an intelligent era [1]. The low power consumption and high photoresponsivity of 6G core devices, and particularly the improvement of detector performance, will facilitate the promotion and reduce the cost of 6G technology. Developing high-performance detectors for the 6G band has become an important issue. Tin diselenide ($SnSe_2$), as an n-type semiconductor with a layered structure of two Se-Sn-Se layers bounded by weak van der Waals interactions, exhibits relatively high intrinsic electron mobility ($462.6\ \mathrm{cm^2 \cdot V^{-1} \cdot s^{-1}}$ at room temperature [2]) and electron affinity (5.2 eV) [3], combined with stability in the air, making it an ideal choice for detectors [4]. With the design of a metal subwavelength structure sandwich semiconductor layer, an electromagnetically induced well (EIW) mechanism is more suitable for $SnSe_2$ (bandgap over the THz wave) to detect THz photons at room temperature. To further improve EIW detector performance, we can combine the advantages of bonding materials and surface plasmon enhancement. Subwavelength field localization can be achieved with surface plasmon polaritons (SPPs), which are usually bound to the surface. A split-ring array structure is often used to introduce SPPs [5, 6]. Considering its thin layer, large area, low noise, low operating voltage, and high efficiency at room temperature, the alumina ceramic interdigital electrode substrate has been used. Alumina ceramic is an ideal substrate material with good thermal conductivity and insulation properties. To reduce noise and exclude the influence of a substrate, in contrast to the other reports using silicon wafers as a substrate, insulated alumina ceramics with an interdigital electrode substrate were chosen to optimize device resistances, reduce the operation voltage, and prevent redundant thermal effect generation. We demonstrated a high-performance room-temperature THz detector based on $SnSe_2$ with an Au split-ring array (Au-SRA) on an alumina ceramic interdigital electrode substrate operation at 6G communication frequencies of 0.1 and 0.28 THz. Considering the EIW and SPPs enhancement combined with the $SnSe_2$ property, our device provides an alternative to developing the large-area, high-performance THz detector toward 6G technology.

Figure 1(a) shows the schematic diagram of the device structure. Large-area $SnSe_2$ film is deposited onto ceramic substrates by magnetron sputtering, and then an Au split-ring array is prepared on the film by magnetron sputtering through masked plates. The $SnSe_2$ layer has a thickness of 220 nm. Subwavelength electromagnetic field localization has attracted considerable attention from researchers [5]. Electromagnetic field localization can increase the coupling between photons and material excitation. Because of the long wavelength, the limitation on the precise size of the device is reduced. Hence, the ultra-strong light-matter coupling regime in the THz range by the split-ring structure has been widely studied [5, 6]. Further investigation of the electric field confinement and surface currents is shown in Figure 1(b). The electric field confinement is revealed in the Au split, as the surface currents remain in the configuration that is highly radiative [6]. Figure 1(c) shows that the carrier movement direction flows along the edge of the split ring and accumulates at the split ring. More design details and test results could be seen in Appendixes A–D. The incident terahertz wave is bound to crack the structure, enhancing the carrier density of the device. Therefore, the detection performance could be enhanced. In addition, the response time of the $SnSe_2$ Au-SRA is shown in Figure 1(d). Accord-

---

* Corresponding author (email: zhangmin@szu.edu.cn, yanpg@szu.edu.cn)

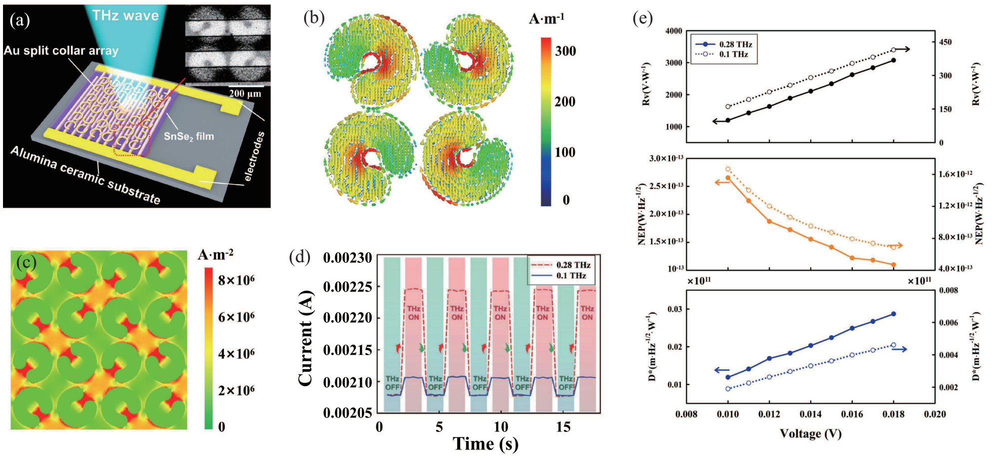

**Figure 1** (Color online) (a) Schematic diagram of devices (inset: SEM picture of the Au split-ring array); (b) surface current distribution and (c) current density of the devices at 0.28 THz; (d) response time of the $SnSe_2$ Au-SRA at 0.1 and 0.28 THz; (e) performance of the Rv, NEP, and D* of the $SnSe_2$ Au-SRA at 0.1 and 0.28 THz.

ing to the experimental results, response time of 90 ms at 0.28 THz and 96 ms at 0.1 THz were obtained. We also compared the THz wave detection performance in Figure 1(e) at the frequencies of 0.1 and 0.28 THz, using the $SnSe_2$ film (as a reference) and a $SnSe_2$ split-ring array. At 0.28 THz (1.07 mm), the Rv values of $SnSe_2$ Au-SRA and $SnSe_2$ film are 3073 and 2824 $V \cdot W^{-1}$, respectively. The measured NEPs are $1 \times 10^{13}$ and $1.2 \times 10^{-13}$ $W \cdot Hz^{-1/2}$, respectively. The performance decrease in low-frequency bands is mainly caused by the interval between the Au-SRA. At 0.1 THz (3 mm), we achieve an Rv, NEP, and D* of 414 $V \cdot W^{-1}$, $6.8 \times 10^{-13}$ $W \cdot Hz^{-1/2}$, and $4.6 \times 10^8$ $m \cdot Hz^{-1/2}$, respectively. The detector exhibits better performance with increasing incident frequency, mainly due to the size and spacing of the split ring in the incident subwavelength range and the stronger binding effect on the high-frequency THz wave by the $SnSe_2$ Au-SRA.

In conclusion, the performance of the THz detector based on $SnSe_2$ Au-SRA on an alumina ceramic interdigital electrode substrate has been demonstrated. The detector possesses a voltage responsivity of up to 3073 $V \cdot W^{-1}$ for the 6G communication frequency of 0.28 THz at room temperature. The detector prototype has been tested under 0.1 and 0.28 THz radiation exposure and shown a responsivity due to the SPP enhancement from 414 to 3073 $V \cdot W^{-1}$. In addition, the NEPs of the devices are $6.8 \times 10^{-13}$ and $1 \times 10^{-13}$ $W \cdot Hz^{-1/2}$ at a relatively low bias of 0.02 V. The response time of 90 ms at 0.28 THz and 96 ms at 0.1 THz were obtained. Our design provides an alternative to developing a large-area, high-performance THz detector and will be a reliable device for use in 6G communication equipment at room temperature.

**Acknowledgements** This work was supported by National Natural Science Foundation of China (Grant No. 12104314).

**Supporting information** Appendixes A–D. The supporting information is available online at info.scichina.com and link.springer.com. The supporting materials are published as submitted, without typesetting or editing. The responsibility for scientific accuracy and content remains entirely with the authors.

## References

1 You X H, Wang C X, Huang J, et al. Towards 6G wireless communication networks: vision, enabling technologies, and new paradigm shifts. Sci China Inf Sci, 2021, 64: 110301

2 Shafique A, Samad A, Shin Y H. Ultra low lattice thermal conductivity and high carrier mobility of monolayer $SnS_2$ and $SnSe_2$: a first principles study. Phys Chem Chem Phys, 2017, 19: 20677–20683

3 Guo C, Guo W L, Xu H, et al. Ultrasensitive ambient-stable $SnSe_2$-based broadband photodetectors for room-temperature IR/THz energy conversion and imaging. 2D Mater, 2020, 7: 035026

4 Chauhan P, Patel A B, Solanki G K, et al. Rhenium substitutional doping for enhanced photoresponse of n-$SnSe_2$/p-Si heterojunction based tunable and high-performance visible-light photodetector. Appl Surf Sci, 2021, 536: 147739

5 Xu X, Xu R, Lin Y S. Tunable terahertz double split-ring metamaterial with polarization-sensitive characteristic. Optics Laser Tech, 2021, 141: 107103

6 Rajabali S, Cortese E, Beck M, et al. Polaritonic nonlocality in light-matter interaction. Nat Photon, 2021, 15: 690–695